Targeted exome sequencing identified a novel *USH2A* mutation in a Chinese Usher syndrome family: a case report

Dongjun Xing
Tianjin Medical University Eye Hospital
Huaiyu Zhou
Tianjin Medical University Eye Hospital
Rongguo Yu
Tianjin Medical University Eye Hospital
Linni Wang
Tianjin Medical University Eye Hospital
Liying Hu
Tianjin Medical University Eye Hospital
Zhiqing Li
Tianjin Medical University Eye Hospital
Xiaorong Li (xiaorli@163.com)
https://orcid.org/0000-0003-0641-2797

Case report

Keywords: Usher syndrome, targeted exome sequencing, mutation, fibronectin type 3 domains

Posted Date: July 29th, 2020

DOI: https://doi.org/10.21203/rs.3.rs-16667/v2

Version of Record: A version of this preprint was published at BMC Ophthalmology on December 10th, 2020. See the published version at https://doi.org/10.1186/s12886-020-01711-7.

Abstract

Background: Usher syndrome is a king of phenotypic and genetic heterogeneous disease. Our purpose was to identify the gene mutation in a Chinese family with Usher syndrome type 2 and describe the clinical features.

Case presentation: A 23-year-old man complained of 10-year nyctalopia and a 3-year decline in visual acuity of both eyes accompanied by congenital dysaudia. To clarify the diagnosis, the clinical symptoms were observed and analysed in combination with comprehensive ophthalmologic examinations as well as genetic analysis (Targeted exome sequencing, TES). Typical clinical presentation of Usher syndrome on fundus was found including a wax yellow-like disc, bone-spicule formations and retinal vessel stenosis. Optical coherence tomography (OCT) and optical coherence tomography angiography (OCTA) showed the loss of ellipsoid zone and the reduction in paracaval vessel density of both eyes. Genetic analysis identified a novel homozygote of c.8483_8486del (p.Ser2828*) in *USH2A*. The mutation of premature translation termination causes the deletion of 19 fibronectin type 3 domains(FN3), transmembrane region (TM) and PDZ-binding motif domain, which plays an important role in protein binding. Combining the clinical manifestation and genetic result, the patient was diagnosed with Usher syndrome type 2.

Conclusions: We found a novel mutation of c.8483_8486del in USH2A gene through TES techniques. The result broaden the spectrum of mutations in Usher syndrome type 2 and suggest that the combination of clinical information and TES molecular diagnosis could help USH patients obtain a better diagnosis.

1 Background

Usher syndrome (USH) is an autosomal recessive disease that is characterized by retinal pigmentosa (RP), sensorineural hearing impairment and vestibule dysfunction. The prevalence is approximately 3.2 to 6.2 per 100,000 [1-4]. It is clinical and genetic heterogeneity. To date, 19 genes and loci are related to USH and atypical USH (RetNet [https://sph.uth.edu/retnet]; October 2019). Among them, 16 genes were identified as causative genes. USH could be divided into three types according to the age of onset, the severity of visual and hearing impairment and vestibule dysfunction. However, due to the point that genetic manifestation is currently not well understood, the rate of missed diagnosis (4%) is high in Asia, especially in China[5].

In patients with USH1, deafness occurs early, and their abnormal visual function is easily ignored. In patients with USH2 and USH3, visual function and hearing abnormalities are gradually progressive. Accurate clinical and molecular diagnoses are the basis of prognosis, treatment selection and eugenics. TES provides us with a new opportunity of revealing the genetic defects in usher syndrome patients[6]. Here, we screened 381 inherited retinal disease (IRD) related genes in a USH2 family and identified a novel mutation of c.8483_8486del (p.Ser2828*) in the *USH2A* gene.

Case presentation

A 23-year-old man visited our clinic and suffered from deafness from childhood with occasional dizziness, nyctalopia for 10 years and visual acuity declined for nearly 3 years of both eyes. Previously, he was diagnosed with "sensorineural deafness" by an otolarynologist. The patient and his family members gave informed consent for the study, which was approved by the Ethics Committee of Tianjin Medical University Eye Hospital (Tianjin, China). Then, peripheral venous blood samples were collected for NGS or Sanger sequencing. For clinical diagnosis, we performed a comprehensive ocular examination that contained best-corrected visual acuity (BCVA), slit-lamp examination, visual field tests, OCT, OCTA, ultra-wide field fundus photography, and fundus autofluorescence (FAF).

2 Methods

DNA Library Preparation

Genomic DNA was extracted from peripheral blood leukocytes of the patient and his family members using the DNA Extraction Kit (TIANGEN, Beijing, China) following the manufacturer's instructions. The DNA was quantified with a Nanodrop 2000 (Thermal Fisher Scientific, DE). A minimum of 3 μg of DNA was used for the indexed Illumina libraries according to the manufacturer's protocol (My Genostics, Inc., Beijing, China). DNA fragments with sizes ranging from 350 bp to 450 bp and those including the adaptor sequences were selected for the DNA libraries.

Targeted Gene Capture and Sequencing

Next, 381 known genes associated with IRD, including USH (Table 1), were selected by a gene capture strategy using the GenCapCustom Enrichment Kit (My Genostics Inc., Beijing, China) following the manufacturer's protocol. The biotinylated capture probes were designed to tile all of the exons with non-repeated regions. Sequencing was performed on an Illumina HiSeq 2000 sequencer (Illumina, San Diego, CA, USA) for paired-end reads of 150 bp.

Bioinformatics Analysis

Following sequencing, raw image files were processed using Bcl2Fastq software (Bcl2Fastq, Illumina, Inc.) for base calling and raw data generation. Low-quality variations (score≥20) were filtered out. The clean reads were then aligned to the reference human genome using Short Oligonucleotide Analysis Package (SOAP) aligner software (SOAP2.21; soap.genomics.org.cn/soapsnp.html) (hg19). After removing polymerase chain reaction (PCR) duplicates using the Picard program, single nucleotide polymorphisms (SNPs) were determined using the SOAP SNP program, and the deletions and insertions (InDels) were detected using Genome Analysis Toolkit software 3.7. Subsequently, we annotated the identified SNPs and InDels with the Exome-assistant program (http://122.228.158.106/exomeassistant)and viewed the short read alignment using MagicViewer to confirm the candidate SNPs and InDels. Non-synonymous variants were evaluated for pathogenicity using Sorting Intolerant From Tolerant [SIFT; (http://sift.jcvi.org/)] and PolyPhen (http://genetics.bwh.harvard.edu/pph2/). Protein Analysis Through Evolutionary Relationships (PANTHER; www.pantherdb.org) and Pathogenic Mutation Prediction (Pmut; http://mmb.pcb.ub.es/PMut/) were also used.

Expanded Validation and Protein Function Prediction

Genomic DNA of the proband was subjected to TES. Filtered candidate variants identified by anIllumina HiSeq 2000sequencer were confirmed by Sanger sequencing. The coding exons containing the detected mutations were amplified using Ex Tag DNA polymerase (Takara, Dalian). The purified PCR samples were sequenced using the ABI PRISM 3730 genetic analyser (Applied Biosystems; Thermo Fisher Scientific, Inc.), and then sequence traces were analysed with the Mutation Surveyor (Softgenetics, PA). The mutation in the family members was confirmed by the same procedure. Multiple sequence alignments were performed using ClustalW2 with the default setting (http://www.ebi.ac.uk/Tools/clustalw2/).Protein structures were determined by SMART (http://smart.emblheidelberg.de). The 3D structure of the protein variation caused by gene mutation was analysed using Protein Data Bank(PDB) and the homology modelling software Swiss-Model. We collected all genomic DNA samples upon informed consent.

3 Results

Clinical Findings

A 23-year-old man presented a 10-year history of deafness and poor night vision. His best corrected visual acuity (BCVA) was 0.6/1.0 (R/L). His parents had a consanguineous marriage, and his grandparents had passed away, but they were healthy according to their past medical history and eye conditions. In addition, his parents and his sister were unaffected (Fig. 1). To better clarify the proband's condition, ophthalmologic investigations were performed. Slit-lamp examination showed that the anterior segment of the eyes was normal. The fundus was typical of RP: the appearance of the wax yellow-like disc, the large amount of osteoblast-like pigmentation, and tapering of the retinal vessels, of which the arteries

were obvious (Fig. 2a). An abnormal parafoveal ring of increased autofluorescence of ultra-wide-angle images was observed, and there was a ring-like hypoautofluorescence region around the macular and optic disc on FAF imaging (Fig. 2b). We also found decreased retinal thickness and absence of the ellipsoid zone in macular (Fig. 2c). Macular OCTA revealed an enlarging foveal avascular area (FAZ) in the superficial capillary plexus and deep capillary plexus, while macular vascular flow density was also decreased (Fig. 3). Examination with Octopus perimeter device put up a tubular visual field in both eyes (Fig. 4).

Genetic and Molecular Analysis

DNA extracted from the peripheral blood was subjected to TES. Genetic tests showed that the patient had a novel mutation (c.8483_8486del) in the USH2A gene. Moreover, DNA samples extracted from proband's sister and parents were used for Sanger sequencing. The results confirmed there was a pedigree genetic co-segregation in this family (Fig. 5a). A model structure for USH2A was generated from homology modelling (Fig. 5b). The mutation resulted in premature translation termination, and the stop-gain variant was predicted to remove 2375 amino acids from the encoded proteins, which would result in truncation of the α-βhydrolase domain (Fig. 5c). This may change the overall function of the folded state of the protein (Fig. 5d).

4 Discussion

We reported the case of a 23-year-old patient who presented a series of typical clinical features with a novel homozygous mutation, p.Ser2828* (rs1199684717) in USH2A, a gene responsible for USH2 (OMIM:276901). The frequency of the mutation is 0.000004 in the Genome Aggregation Database and it's found at heterozygous state in one European non Finnish individual. Mutations in *USH2A* are associated with USH2, it is responsible for almost 50% of USH cases[7].

USH2A codes two alternatively spliced isoforms of usherin. Short ~170 kDa isoform a, consisting of 21 exons, is regarded as an extracellular protein. Full-length ~580 kDa isoform b is a complex transmembrane protein composed of three regions: a large extracellular region consisting of an N-terminal signal peptide, laminin G-like domain (LamGL), laminin domain N-terminal (LamNT), laminin-type EGF-like modules (EGF-Lam), fibronectin type III (FN3) repeats, laminin G domains (LamG); a transmembrane region(TM); and a cytoplasmic C-terminal domain containing a PDZ-binding motif[8, 9]. Usherin is distributed in the periciliary membrane complex and synapse in photoreceptors. All USH1 and USH2 proteins are organized as protein networks by the scaffold proteins harmonin (USH1C), whirlin (USH2D) and SANS (USH1G). Usherin(*USH2A*) and VLGR1b(*USH2C*) are part of the links that are intracellularly attached to the scaffold proteins. On the other hand, during the differentiation of the hair bundle, both USH1 and USH2 proteins contribute to the formation of side links located at the tip and the base of the stereocilia, respectively. They exist in multiprotein complexes that work together as molecular networks to anchor them to the stereocilia actin filaments[10-14].

The homozygous mutation (p.Ser2828*) in *USH2A* made the premature termination translation, as a result, 19 FN3, TM and PDZ-binding motif domains were deleted. FN3 plays a key role in cell adhesion, cell morphology, thrombosis, cell migration, and embryonic differentiation and pathophysiologic processes such as angiogenesis and vascular remodeling[15]. TM exists at the base of the differentiating stereocilia, and it makes up the mechanosensitive hair bundles receptive to sound. PDZ-binding motif domains provide the anchoring of interstereocilia lateral links to the F-acin core of stereocilia[16]. In this regard, we suppose that the absence these domains corresponding to the incompleteness of usherin, which might probably have in turn affected the process of stereocilia differentiation and maturation, resulting in a milder stereocilia dysmorphic phenotype. Several positions are found associated exclusively with pathogenic of FN3 in usherin[17], which support our hypothesis. However, the pathway needs to be confirmed by molecular experiments in the future.

Whole-genome sequencing (WGS), whole-exome sequencing (WES) and TES is three major methodologies for molecular diagnosis of IRD. WGS is useful for detecting copy number variations and structural variations[18]. WES is especially useful for identifying novel IRD related genes. TES is an accurate, rapid and cost-effective approach for screening of multiple genes[19], but still have some major limitations, such as detecting variants in low-depth regions and copy number variations[18, 20]. Because of the higher cost, both of the WGS and WES is less widely used than TES. TES is suitable for molecular diagnosis of USH. As the great diversity of various types of pathogenic genes and the frequent occurrence of new mutations, array-based diagnosis often could not accurately reflect the pathogenicity. USH pathogenic genes have many subtypes and numerous exons. At present, more than 400 coding exons have been commented.[21] Therefore, a higher diagnosis rate can be obtained by using sequence-based diagnosis method.

Conclusion

Here, we report a novel homozygous mutation, c.8483_8486del, in the *USH2A* gene through TES techniques. The mutation truncated the translation of the *USH2A* gene, and 19 FN3, TM and PDZ-binding motif domain were lost, which influenced the function of stereocilia. We broadened the spectrum of mutations in the disease and provided a new locus for gene therapy of the disease. The combination of TES molecular diagnosis and clinical information can help USH patients obtain more accurate diagnoses.

Declarations

Ethics approval and consent to participate

This study adhered to the tenets of the Declaration of Helsinki and was approved by institution review board of Tianjin Medical University Eye Hospital(Tianjin, China), Number：2019KY-02. The

written informed consent to participate was obtained from the patients.

Consent to publication

Written informed consent for publication of their clinical images and genetic results in this manuscript was obtained from the patients according to Ethic Committee Regulations.

Availability of data and materials

All data are fully available without restriction.

Competing interests

The authors declare that they have no competing interests.

Fundings

This study was supported by Natural Science Foundation of Tianjin City (Award number: 17JCYBJC27200; Recipient: Zhiqing Li) and Tianjin Clinical Key Subject Construction Project (Award number: TJLCZDXKQ022; Recipient: Dongjun Xing) in China.

Author Contributions

XL and ZL conceived the idea and take responsibility for the integrity of the data. DX and HZ collected the samples, performed data analyses and wrote the manuscript. Both of authors also contributed equally to this work. RY, LW and LH performed the experiments. All authors have read and approved the final manuscript.

Acknowledgements

We thank all the family members for their participation in this study.

Abbreviations

USH: Usher syndrome; OCT: Optical coherence tomography; OCTA: Optical coherence tomography angiography; IRD: inherited retinal disease; FN3: Fibronectin type 3 domains; TES: Targeted exome sequencing; RP: retinal pigmentosa; BCVA: best-corrected visual acuity; FAF: fundus autofluorescence; SOAP: Short Oligonucleotide Analysis Package; SNPs: single nucleotide polymorphisms; PCR: polymerase chain reaction; PDB: Protein Data Bank; FAZ: foveal avascular area; LamGL: laminin G-like domain; LamNT: laminin domain N-terminal; EGF-Lam: laminin-type EGF-like modules; LamG: laminin G domains

References

1. Blanco-Kelly F, Jaijo T, Aller E, et al. Clinical aspects of Usher syndrome and the USH2A gene in a cohort of 433 patients. *JAMA Ophthalmol*. 2015;133(2):157-64.
2. Cohen M, Bitner-Glindzicz M, Luxon L. The changing face of Usher syndrome: clinical implications. *Int J Audiol*. 2007;46(2):82-93.
3. Hartel BP, Löfgren M, Huygen PL, et al. A combination of two truncating mutations in USH2A causes more severe and progressive hearing impairment in Usher syndrome type IIa. *Hear Res*. 2016;339:60-8.
4. Hope CI, Bundey S, Proops D, Fielder AR. Usher syndrome in the city of Birmingham--prevalence and clinical classification. *Br J Ophthalmol*. 1997;81(1):46-53.
5. Pehere NK, Khanna RC, Marlapati R, Sannapaneni K. Prevalence of ophthalmic disorders among hearing-impaired school children in Guntur district of Andhra Pradesh. Indian J Ophthalmol. 2019. 67(4): 530-535.
6. Huang, X.F., et al., 2013. Targeted exome sequencing identified novel USH2A mutations in Usher syndrome families. PLoS ONE 8 (5), e63832.
7. Jouret G, Poirsier C, Spodenkiewicz M, et al. Genetics of Usher Syndrome: New Insights From a Meta-analysis. *Otol Neurotol*. 2019;40(1):121-129.
8. Méndez-Vidal C, González-Del Pozo M, Vela-Boza A, et al. Whole-exome sequencing identifies novel compound heterozygous mutations in USH2A in Spanish patients with autosomal recessive retinitis pigmentosa. *Mol Vis*. 2013;19:2187-95.
9. Pierrache LH, Hartel BP, van Wijk E, et al. Visual Prognosis in USH2A-Associated Retinitis Pigmentosa Is Worse for Patients with Usher Syndrome Type IIa Than for Those with Nonsyndromic Retinitis Pigmentosa. *Ophthalmology*. 2016;123(5):1151-60.
10. Bonnet C, El-Amraoui A. Usher syndrome (sensorineural deafness and retinitis pigmentosa): pathogenesis, molecular diagnosis and therapeutic approaches. *Curr Opin Neurol*. 2012;25(1):42-9.
11. Cosgrove D, Zallocchi M. Usher protein functions in hair cells and photoreceptors. *Int J Biochem Cell Biol*. 2014;46:80-9.
12. Sorusch, N., et al., 2014. Usher syndrome protein network functions in the retina and their relation to other retinal ciliopathies. Adv. Exp. Med. Biol. 801 527-533.
13. Mathur, P., Yang, J., 2015. Usher syndrome: Hearing loss, retinal degeneration and associated abnormalities. Biochim. Biophys. Acta 1852 (3), 406-420.
14. Kremer, H., et al., 2006. Usher syndrome: molecular links of pathogenesis, proteins and pathways. Hum. Mol. Genet. 15 Spec No 2 R262-270.

15. Maurer LM, Ma W, Mosher DF. Dynamic structure of plasma fibronectin. *Crit Rev Biochem Mol Biol*. 2015;51(4):213-27.
16. Adato A, Lefèvre G, Delprat B, Michel V, Michalski N, Chardenoux S, et al. Usherin, the defective protein in Usher syndrome type IIA, is likely to be a component of interstereocilia ankle links in the inner ear sensory cells. Hum Mol Genet. 2005;14(24):3921-32. doi:10.1093/hmg/ddi416.
17. Baux D, Blanchet C, Hamel C, et al. Enrichment of LOVD-USHbases with 152 USH2A genotypes defines an extensive mutational spectrum and highlights missense hotspots. Hum Mutat. 2014. 35(10): 1179-86.
18. Huang XF, Mao JY, Huang ZQ, et al. Genome-Wide Detection of Copy Number Variations in Unsolved Inherited Retinal Disease. Invest Ophthalmol Vis Sci. 2017. 58(1): 424-429.
19. Huang XF, Wu J, Lv JN, Zhang X, Jin ZB. Identification of false-negative mutations missed by next-generation sequencing in retinitis pigmentosa patients: a complementary approach to clinical genetic diagnostic testing. Genet Med. 2015. 17(4): 307-11.
20. Huang XF, Huang F, Wu KC, et al. Genotype-phenotype correlation and mutation spectrum in a large cohort of patients with inherited retinal dystrophy revealed by next-generation sequencing. Genet Med. 2015. 17(4): 271-8.
21. Jiang L, Liang X, Li Y, et al. Comprehensive molecular diagnosis of 67 Chinese Usher syndrome probands: high rate of ethnicity specific mutations in Chinese USH patients. *Orphanet J Rare Dis*. 2015;10:110.

Table

Table 1 List of 381 genes chosen for targeted gene capture

ABCA4	ADAMTSL4	ALMS1	ARMS2	BBS12	BLOC1S6	C5AR2	CAPN5
CEP290	CFI	CLRN1	COL11A1	CRX	CYP4V2	DTNBP1	ERCC8
FSCN2	GNB3	GUCA1B	HK1	HTRA1	IMPG2	KIAA1549	LRIT3
MAPKAPK3	MKS1	NDP	NRL	OPN1MW2	PCDH15	PDE6H	PEX16
PEX7	PNPLA6	PRPF31	RABGGTA	RD3	RIMS1	RPGR	SEMA4A
SLC25A15	SPATA7	TENM3	TMEM231	TRPM1	TUBGCP4	USH2A	YAP1
ABCB6	ADGRA3	ANO5	ASRGL1	BBS2	BMP4	C5orf42	CC2D2A
CEP41	CHM	CLUAP1	COL11A2	CSPP1	DHCR7	EFEMP1	EXOSC2
FXN	GNPTG	GUCY2D	HMCN1	IDH3B	INPP5E	KIF11	LRP5
MC1R	MLPH	NEK2	NYX	OPN1SW	PCYT1A	PDZD7	PEX19
PGK1	POC1B	PRPF4	RABGGTB	RDH11	RLBP1	RPGRIP1	SGCD
SLC26A4	SPP2	TIMP3	TMEM237	TSPAN12	TUBGCP6	VCAN	ZNF408
ABCC6	ADGRV1	AP3B1	ATF6	BBS4	C10orf11	C8orf37	CCDC28B
CEP78	CIB2	CNGA1	COL18A1	CST3	DHDDS	ELOVL4	EYA1
FZD4	GPR143	GUSB	HMX1	IDUA	INVS	KIF7	LRPAP1
MCOLN1	MPDZ	NMNAT1	OAT	OR2W3	PDCD2	PEX1	PEX2
PGR	POMGNT1	PRPF6	RAX	RDH12	ROM1	RPGRIP1L	SHH
SLC38A8	STRA6	TINF2	TMEM67	TTC21B	TULP1	VHL	ZNF423
ABHD12	ADIPOR1	APOE	ATOH7	BBS5	C1QTNF5	C9	CDH23
CERKL	CLDN19	CNGA3	COL2A1	CTC1	DHX38	ERCC2	EYS
GDF3	GPR179	HARS	HPS1	IFT140	IQCB1	KIZ	LYST
MERTK	MTHFR	NPHP1	OCA2	OTX2	PDE6A	PEX10	PEX26
PHYH	PPT1	PRPF8	RAX2	RDH5	RP1	RS1	SHOX
SLC39A5	TBK1	TLR3	TMEM98	TTC8	TYR	VPS13B	ZNF513
ACBD5	AGBL5	ARL13B	ATXN7	BBS7	C2	CA4	CDH3
CFB	CLN3	CNGB1	COL4A1	CTNNA1	DMD	ERCC3	FAM161A
GDF6	GRK1	HEXA	HPS3	IFT172	ITGA2B	KLHL7	LZTFL1
MFRP	MTTP	NPHP3	OFD1	P3H2	PDE6B	PEX11B	PEX3
PITPNM3	PRCD	PRPH2	RB1	RGR	RP1L1	SAG	SIX5
SLC45A2	TCTN1	TLR4	TOPORS	TTLL5	TYRP1	VSX2	ZNF644
ACO2	AHI1	ARL2BP	BBIP1	BBS9	C21orf2	CABP4	CDHR1
CFH	CLN5	CNGB3	COL9A1	CTSD	DNAJC5	ERCC4	FBLN5
GMPPB	GRM6	HEXB	HPS4	IFT27	ITGB3	LAMA1	MAK
MFSD8	MVK	NPHP4	OPA3	PANK2	PDE6C	PEX12	PEX5

PLA2G5	PRDM13	PRSS56	RBP3	RGS9	RP2	SALL2	SIX6
SLC7A14	TCTN2	TMEM126A	TPP1	TTPA	UNC119	WDPCP	ADAM9
AIPL1	ARL3	BBS1	BEST1	C2orf71	CACNA1F	CEP164	CFHR1
CLN6	CNNM4	COL9A2	CTSF	DRAM2	ERCC5	FBN2	GNAT1
GRN	HFE	HPS5	IMPDH1	ITM2B	LCA5	MAN2B1	MITF
MYO5A	NR2E1	OPN1LW	PAX2	PDE6D	PEX13	PEX5L	PLEKHA1
PROM1	RAB27A	RBP4	RGS9BP	RP9	SCO2	SLC24A1	SNRNP200
TCTN3	TMEM138	TRIM32	TTR	USH1C	WDR19	ADAMTS18	ALDH1A3
ARL6	BBS10	BLOC1S3	C3	CACNA2D4	CEP250	CFHR3	CLN8
CNOT9	CRB1	CX3CR1	DTHD1	ERCC6	FLVCR1	GNAT2	GUCA1A
HGSNAT	HPS6	IMPG1	KCNV2	LRAT	MANBA	MKKS	MYO7A
NR2E3	OPN1MW	PAX6	PDE6G	PEX14	PEX6	PLK4	PRPF3
RAB28	RCBTB1	RHO	RPE65	SDCCAG8	SLC24A5	SOD1	TEAD1
TMEM216	TRNT1	TUB	USH1G	WHRN	-	-	-

Figures

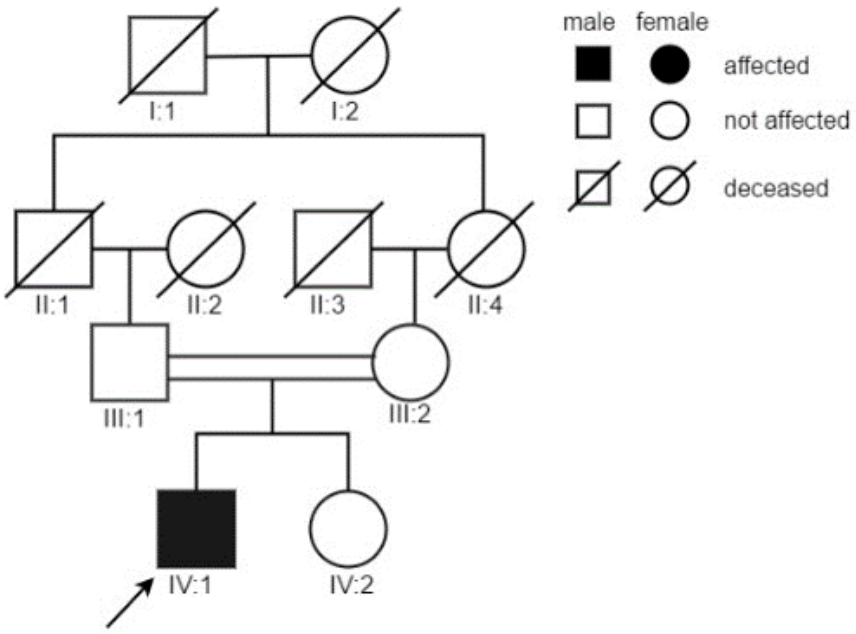

Figure 1

Pedigree of the family

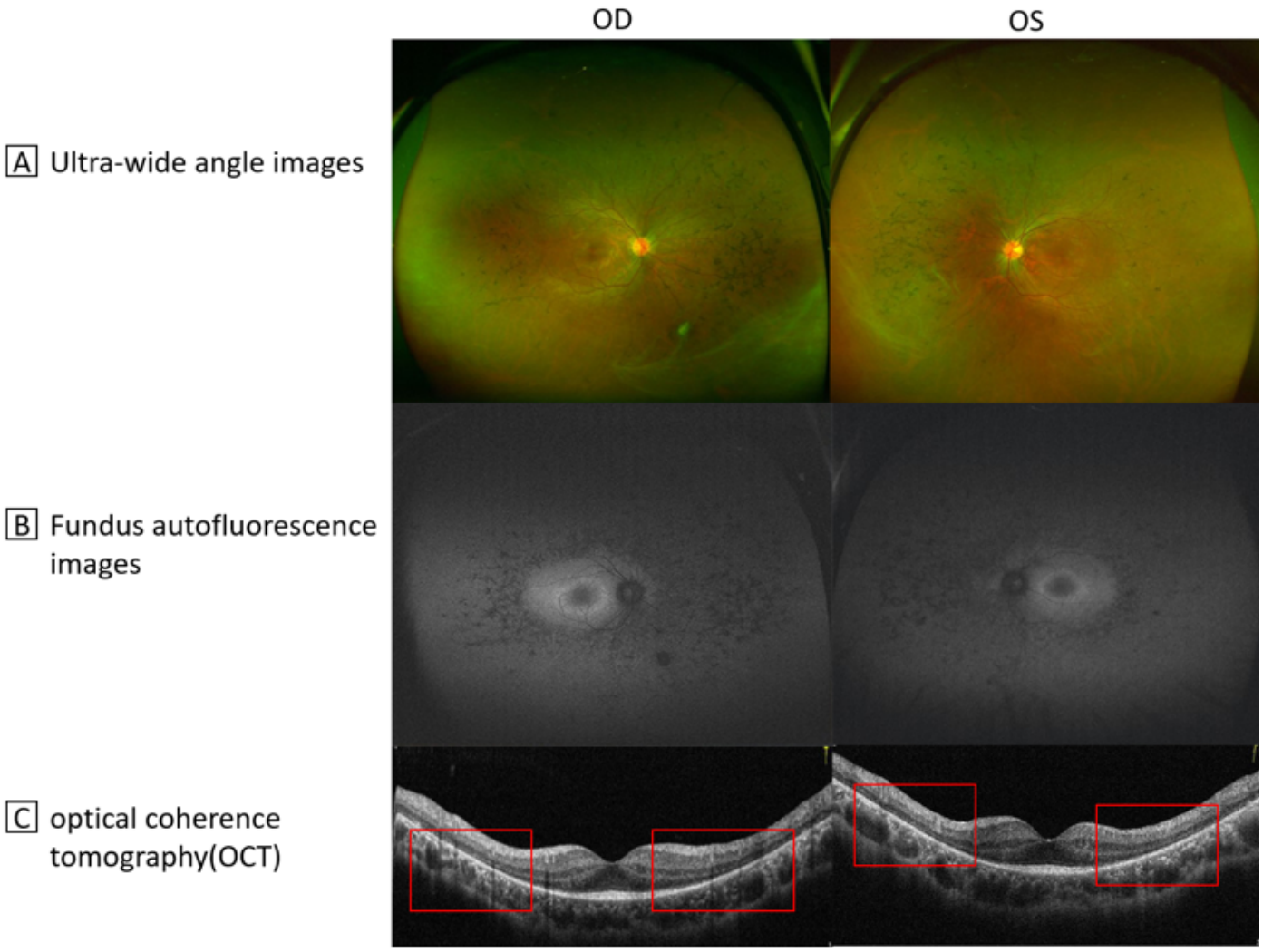

Figure 2

Ultra-wide angle images of patient demonstrated midperipheral retinal atrophy and pigment migration and attenuated retinal vessels (a). FAF demonstrated midperipheral patchy hypoautofluorescence with a parafoveal autofluorescent ring (b). OCT demonstrated loss of the ellipsoid zone consistent with atrophy of the outer nuclear layer outside the hyperautofluorescent ring on FAF(red line) (c)

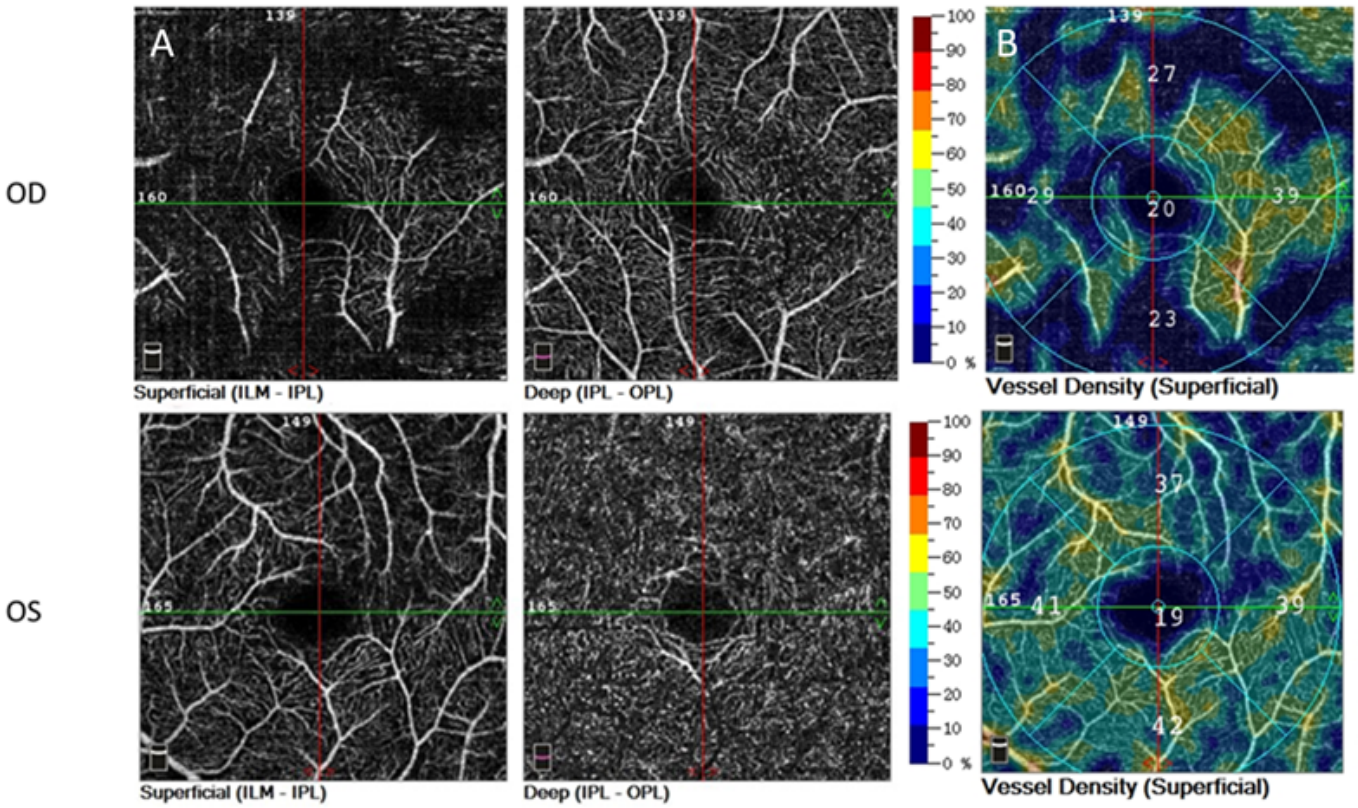

Figure 3

Macular OCTA images demonstrated an enlarging FAZ in both superficial capillary plexus and deep capillary plexus (a). macular vascular flow density(superficial) decreased in both eye (b)

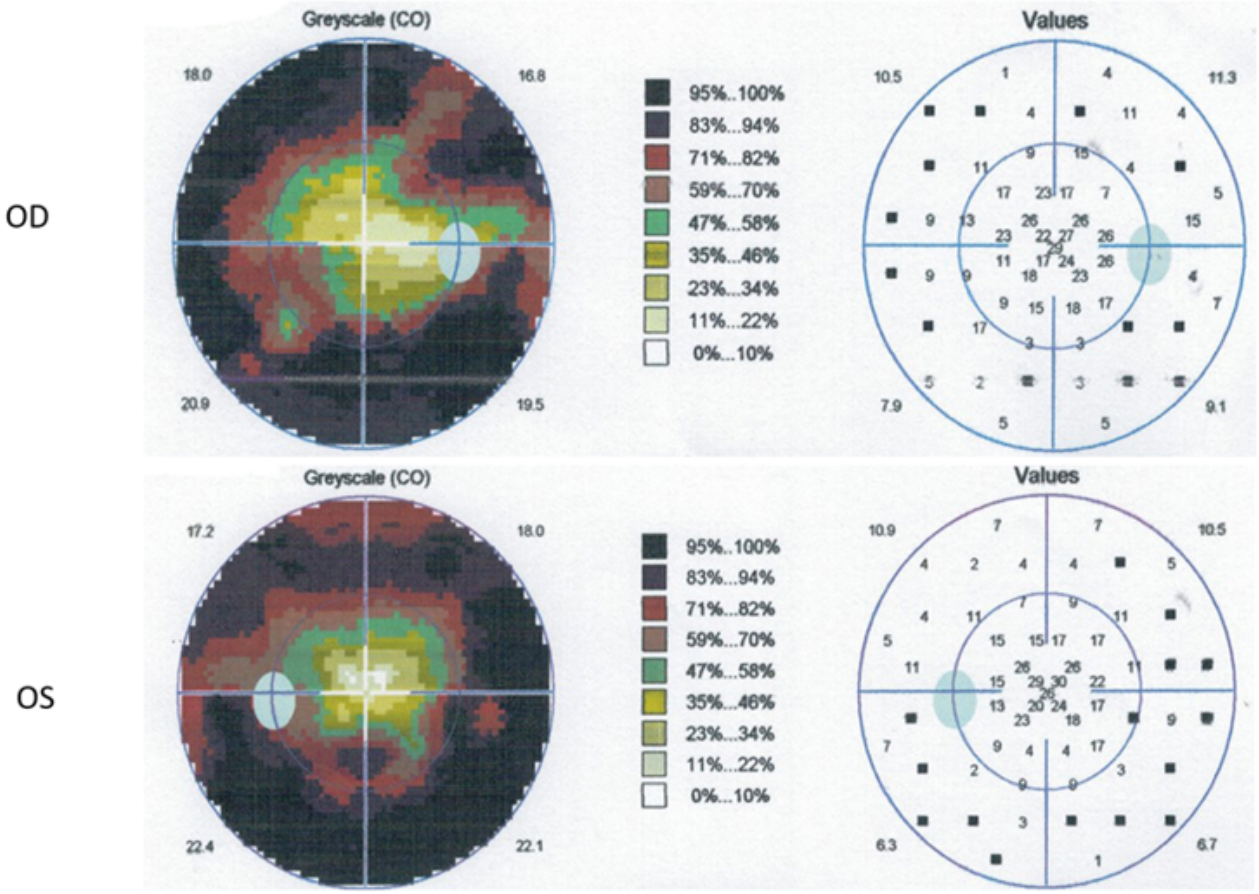

Figure 4

Octopus Visual Field of the patient demonstrated a described visual field constriction in each eye.

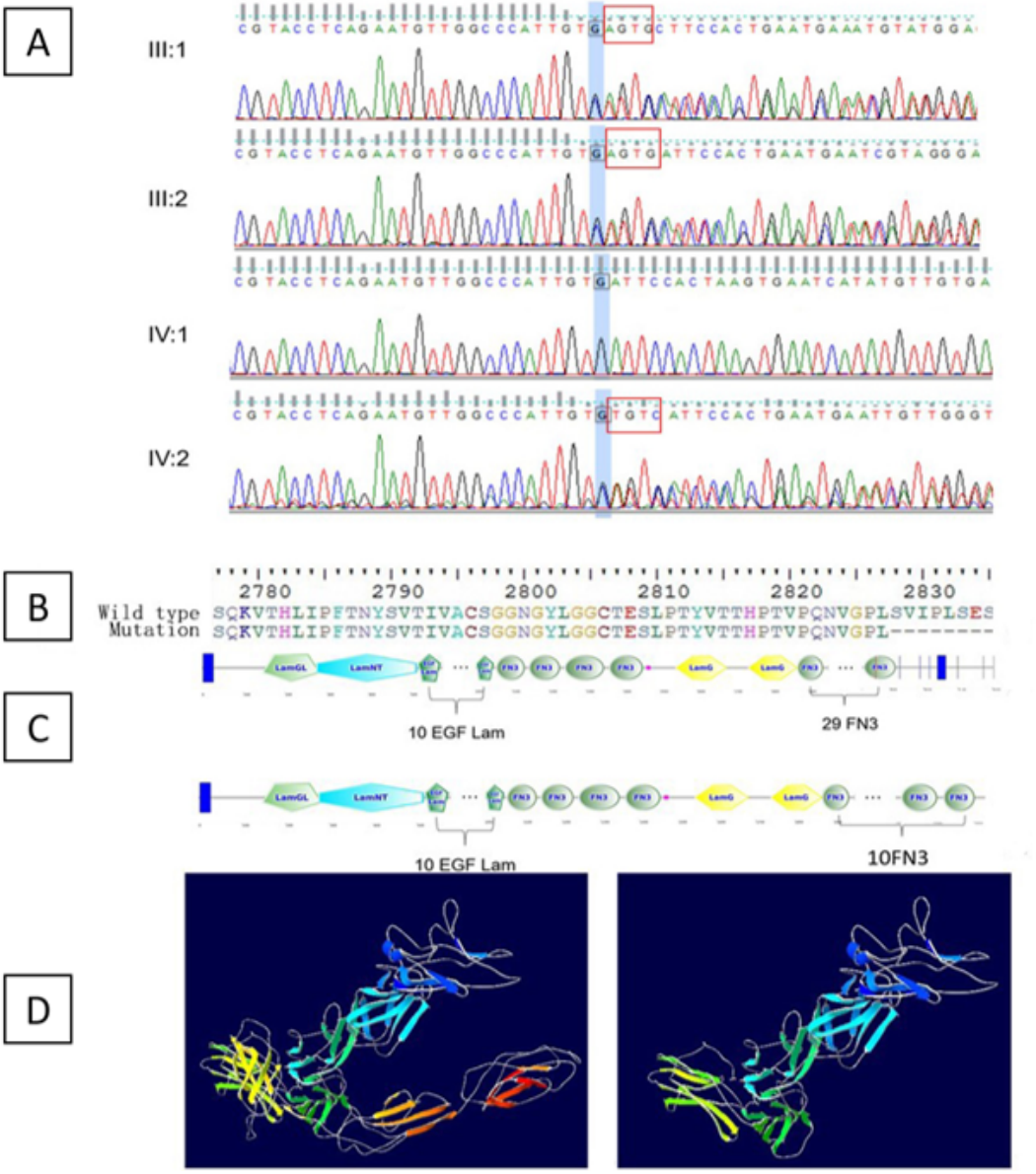

Figure 5

Identified mutation confirmed by Sanger sequencing. Ⅲ:1 (the patient) harbored a homozygous mutation (c.8483_8486del/c.8483_8486del), Ⅳ1, Ⅳ2 and Ⅳ:1 were identified with a heterozygous mutation (c.8483_8486del/-) (a). The amino acid sequence of the mutant usherin (b). It's the tertiary structure of usherin, and 19 FN3, TM and PDZ-binding motif domains were lost in the truncated protein. (c). The change of the folded state of the protein (d)